

# *ROSAT* HRI observations of the Local Group galaxies IC 10, NGC 147 and NGC 185

W.N. Brandt,<sup>1,2\*</sup> M.J. Ward,<sup>3</sup> A.C. Fabian<sup>2</sup> and P.W. Hodge<sup>4</sup>

<sup>1</sup>*Harvard-Smithsonian Center for Astrophysics, 60 Garden Street, Cambridge, Massachusetts 02138, USA*

<sup>2</sup>*Institute of Astronomy, Madingley Road, Cambridge CB3 0HA*

<sup>3</sup>*X-ray Astronomy Group, Department of Physics & Astronomy, University of Leicester, University Road, Leicester LE1 7RH*

<sup>4</sup>*Department of Astronomy, Box 351580, University of Washington, Seattle, Washington 98195, USA*

23 September 2018

## ABSTRACT

We report on pointed X-ray observations of IC 10, NGC 147 and NGC 185 made with the *ROSAT* High Resolution Imager (HRI). These are three Local Group galaxies that have never been previously studied in detail in the X-ray regime. IC 10 is the closest starburst galaxy to our own Galaxy, and NGC 147 and NGC 185 are companions to M31. We have discovered a variable X-ray source coincident with IC 10. The source is located near the centre of a large, non-thermal bubble of radio emission, and it is positionally coincident with an emission line star in IC 10 which has been classified as a WN type Wolf-Rayet star. We demonstrate that a confusing foreground or background source is improbable. The X-ray source is probably an X-ray binary in IC 10, and it may be a Wolf-Rayet + black hole binary. The source has mean and maximum 0.1–2.5 keV isotropic luminosities of about 2 and 4 times  $10^{38}$  erg s<sup>-1</sup>. We do not detect any sources in the central regions of NGC 147 or NGC 185. We place upper limits on their central X-ray emission, and we list all X-ray sources coincident with their outer extents. We also present the first X-ray detections of the well-studied Algol-type binary TV Cas and the W UMa-type binary BH Cas, which were both serendipitously observed during our IC 10 pointing.

**Key words:** galaxies: individual: IC 10 – galaxies: individual: NGC 147 – galaxies: individual: NGC 185 – stars: individual: TV Cas – stars: individual: BH Cas – X-rays: galaxies – X-rays: stars.

## 1 INTRODUCTION

IC 10 is a small irregular galaxy in the Local Group (see Hodge 1994 for a brief history and references). It is rich in newly formed massive blue stars and is peppered with over 140 H II regions (Hodge & Lee 1990). Recently, Massey, Armandroff & Conti (1992) and Massey & Armandroff (1995) have identified 15 Wolf-Rayet stars in IC 10. Since Wolf-Rayet stars are descended from only the most massive ( $\gtrsim 30\text{--}40 M_{\odot}$ ) stars, this argues that IC 10 has an unusually large unevolved massive (OB) star population as well, with a *galaxy-wide* surface density of massive stars that is higher by a factor of 2 than any other Local Group galaxy. The galaxy-wide massive star density of IC 10 is comparable

to that observed in isolated regions of recent star formation in other Local Group galaxies, in accord with earlier suggestions that IC 10 is currently undergoing a starburst.

The radio continuum emission from IC 10 is strong (e.g. Klein & Gräve 1986). Of particular relevance to this work is the fact that Yang & Skillman (1993; hereafter YS93) have discovered a non-thermal bubble of radio emission in IC 10. This bubble has a diameter of about 250 pc, and comparison with data at other wavelengths shows that it is associated with a region of star formation as well as the densest H I concentration in IC 10. YS93 argue that the bubble is a collection of supernova remnants (i.e. a ‘super-bubble’). The 408 MHz radio luminosity of the bubble is about 2.6 times that of N132D, one of the brightest supernova remnants (SNR) in the Large Magellanic Cloud. IC 10 also has two H<sub>2</sub>O maser complexes which include a flaring megamaser as well as a maser with intraday variability (e.g. Argon et al. 1994; Baan & Haschick 1994).

\* Current address: The Pennsylvania State University, Department of Astronomy and Astrophysics, 525 Davey Lab, University Park, Pennsylvania 16802, USA

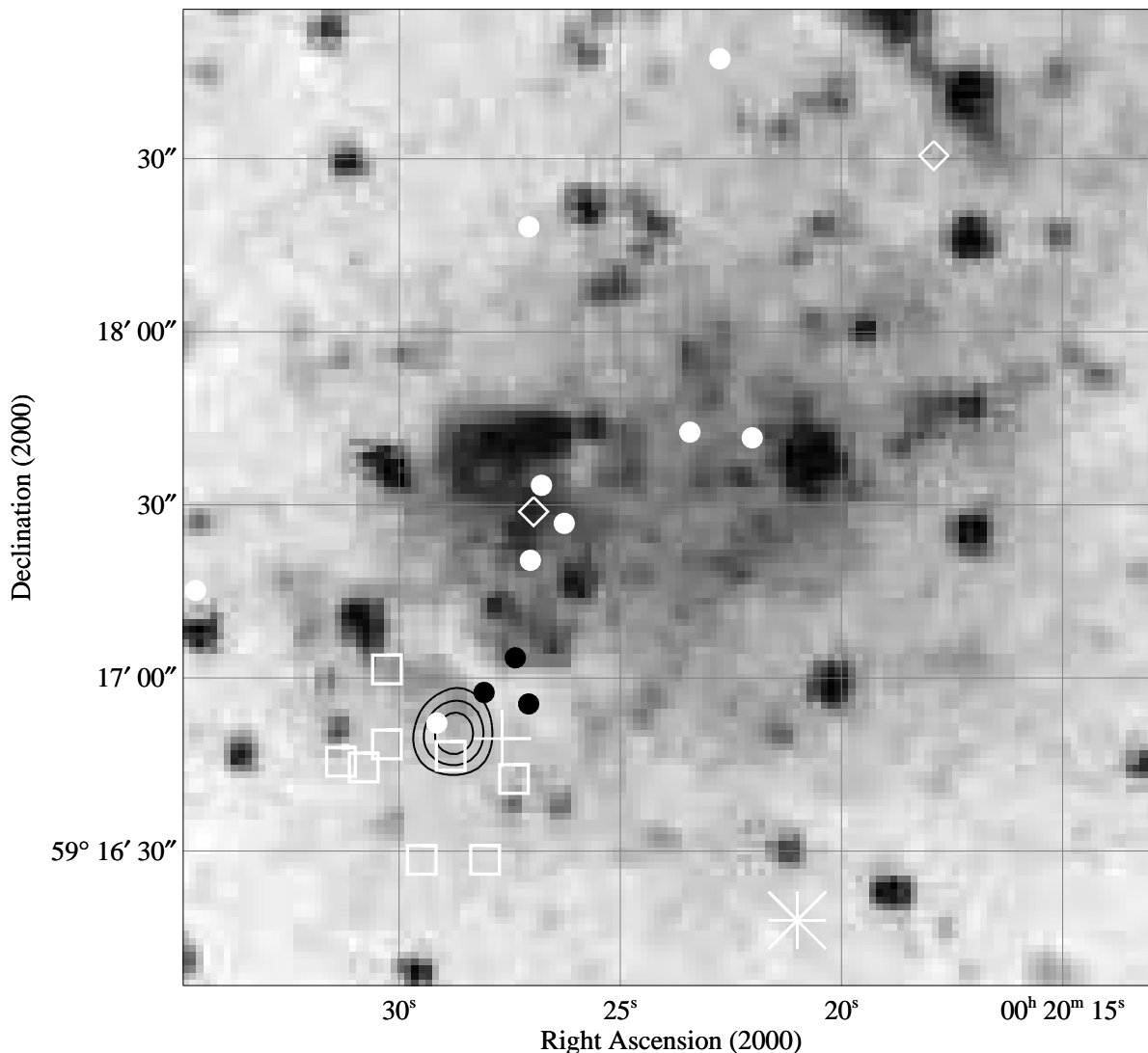


**Figure 1.** Contours of the HRI image of IC 10 overlaid on the image from the Palomar Schmidt  $B_J$  plate. Contours are in black and are at 44.8, 67.1 and 89.5 per cent of the maximum pixel value (see the text for absolute normalization). White solid dots show the positions of probable Wolf-Rayet stars from Massey & Armandroff (1995), and black solid dots show the positions of molecular clouds from Wilson (1995). Diamonds show the positions of maser complexes, and squares show the positions of SNR candidates from table 3 of YS93. The cross shows the central position of H II region # 113 from Hodge & Lee (1990) after correcting for the offset given in Ohta et al. (1992). The star shows the revised centroid position of the all-sky survey source, as described in the text (Th. Boller, private communication). Note that our HRI source is near the centre of the YS93 non-thermal radio superbubble (compare with Figure 3) and coincident with the claimed Wolf-Rayet star WR17.

Due to the fact that IC 10 is the closest starburst galaxy to our own Galaxy and has interesting properties at a variety of wavelengths, we performed a deep pointing towards it with the HRI detector (David et al. 1995) on *ROSAT* (Trümper 1983). Our main goals were to look for X-ray binaries, strong SNR, evidence for a hot interstellar medium and any X-ray emission near the maser complexes. This is the first pointed X-ray observation of IC 10 to our knowledge.

Distance estimates to IC 10 range from 0.7–3 Mpc, although a consensus is developing that the distance is  $\approx 1$

Mpc (see Massey & Armandroff 1995). We shall adopt this distance, for which the HRI spatial resolution of  $\approx 5$  arcsec corresponds to  $\approx 24$  pc. The Galactic column density towards IC 10 is high due to its low Galactic latitude, and IC 10 almost certainly has significant intrinsic absorption (see below). From the data of Stark et al. (1992), we obtain a Galactic column density of  $\approx 3.2 \times 10^{21} \text{ cm}^{-2}$ . This column blocks almost all photons with energies  $\lesssim 0.4$  keV.

NGC 147 and NGC 185 are a pair of dwarf elliptical galaxies that are about 100 kpc from M31. NGC 147 has a predominantly old stellar population ( $\gtrsim 12$  Gyr) and 4

known globular clusters. Its H I content is low. Most of the stars in NGC 185 are also old, but in addition it has OB stars, dust clouds and a fairly massive amount of H I in its interstellar medium. It probably contains a SNR (Gallagher, Hunter & Mould 1984), and it has 6 known globular clusters. Unlike NGC 205, NGC 185 is too far from M31 to have had its star formation triggered by a recent interaction with this galaxy. Hodge (1994) gives further details about these galaxies and references to the literature. Helfand (1984) suggested that each of these galaxies might have  $\sim 2$  X-ray binaries (see his table 1), so we performed *ROSAT* HRI pointings towards them. We also wanted to look for any evidence of a hot galactic wind, as discussed in section IVb of Ford, Jacoby & Jenner (1977). For these galaxies we adopt a distance of 600 kpc and a Galactic column of  $\approx 1.2 \times 10^{21} \text{ cm}^{-2}$  (Stark et al. 1992).

## 2 OBSERVATIONS AND DATA ANALYSIS

### 2.1 IC 10

#### 2.1.1 Observation and X-ray image details

IC 10 was observed with the *ROSAT* HRI starting on 1996 January 18 (RH600902: total raw exposure of 32.7 ks spread over 10.8 days). The *ROSAT* observation was performed in the standard ‘wobble’ mode, and reduction and analysis of the resulting data were performed with the Starlink ASTERIX X-ray data processing system.

In Figure 1 we show contours of part of the full band ( $\approx 0.1$ – $2.5$  keV) HRI image overlaid on the image of IC 10 from the Palomar Schmidt  $B_J$  plate [see Minkowski & Abell 1963 for more information on the optical image]. We also show the positions of interesting objects in IC 10 identified at other wavelengths (see the figure caption).

We have checked the astrometry of the HRI image using a bright star that is also the brightest X-ray source in the field, and it appears to be nominal (see Figure 2). This star is identified as TV Cas (HD 1486;  $V = 7.3$ ; orbital period of 1.81 days), a well-studied, Algol-type, eclipsing binary (see Khalessheh & Hill 1992 and references therein). In addition, we have also detected the W UMA-type binary BH Cas ( $V = 12.3$ ; orbital period of  $\sim 0.39$  days; see Metcalfe 1995 and references therein). The X-ray and SIMBAD database positions for BH Cas agree to within 3 arcsec, further confirming the HRI astrometry. These are the first X-ray detections of TV Cas and BH Cas to our knowledge, and we give their X-ray details in Appendix A.

#### 2.1.2 IC 10 X-1

##### Basic observed X-ray properties

The HRI image shows a clear detection of a pointlike source coincident with IC 10 (hereafter referred to as IC 10 X-1), and we have used the ASTERIX point source searching program PSS (Allan 1995) to quantify the source properties. The centroid position of X-1 is  $\alpha_{2000} = 00^{\text{h}} 20^{\text{m}} 29.0^{\text{s}}$ ,  $\delta_{2000} = 59^{\circ} 16' 50.4''$ , with an error radius (statistical plus systematic) of approximately 5 arcsec. The source has  $261 \pm 18$  counts (after background subtraction), giving a mean HRI

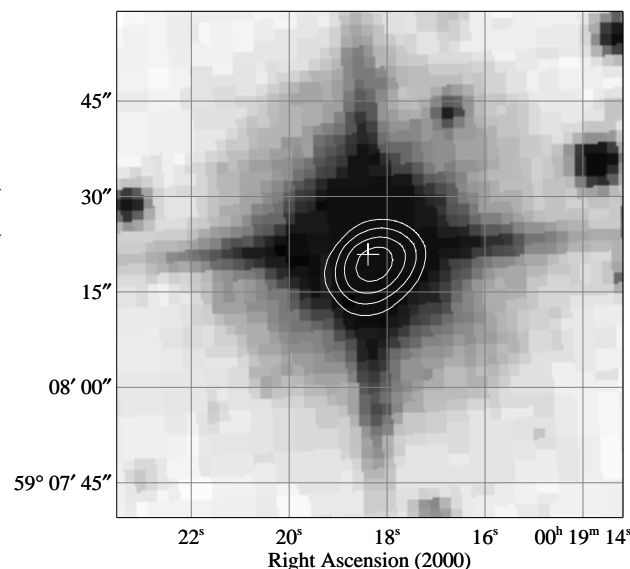


**Figure 2.** Contours of part of our HRI image near TV Cas overlaid on the image from the Palomar Schmidt  $B_J$  plate. Contours are at 58.1, 69.8, 81.4 and 93.0 per cent of the maximum pixel value (see Appendix A for absolute normalization). The cross shows the position of TV Cas from the SIMBAD database ( $\alpha_{2000} = 00^{\text{h}} 19^{\text{m}} 18.4^{\text{s}}$ ,  $\delta_{2000} = 59^{\circ} 08' 20.9''$ ). Note that the HRI contours are well aligned with the star, confirming the HRI astrometry.

count rate of  $7.9 \times 10^{-3} \text{ count s}^{-1}$ . The detection statistical significance is  $> 25\sigma$ . It is possible to use PIMMS (Mukai 1995) and a spectral model to convert the observed mean HRI count rate into a mean source flux. We adopt a power-law model with a photon index of  $\Gamma = 2$ . The Galactic column density is  $3.2 \times 10^{21} \text{ cm}^{-2}$ , and if we adopt this column density we obtain a power-law normalization of  $2.4 \times 10^{-4}$  photons  $\text{cm}^{-2} \text{ s}^{-1} \text{ keV}^{-1}$  at 1 keV and a 0.1–2.5 keV absorbed flux of  $3.3 \times 10^{-13} \text{ erg cm}^{-2} \text{ s}^{-1}$ . The 0.1–2.5 keV absorbed flux is not a strong function of the adopted column density. For example, if we use a much lower column of  $5 \times 10^{20} \text{ cm}^{-2}$ , then we obtain a power law normalization of  $1.1 \times 10^{-4}$  photons  $\text{cm}^{-2} \text{ s}^{-1} \text{ keV}^{-1}$  at 1 keV and a 0.1–2.5 keV absorbed flux of  $3.0 \times 10^{-13} \text{ erg cm}^{-2} \text{ s}^{-1}$ . We estimate absorption-corrected fluxes and luminosities below, after we have considered how likely it is that X-1 is indeed associated with IC 10.

We have searched the literature for sources at other wavelengths that are coincident with the detected X-ray source, and we find that the X-ray source lies in the middle of a hive of activity in IC 10. YS93 quote an approximate central position for their non-thermal radio superbubble of  $\alpha_{2000} = 00^{\text{h}} 20^{\text{m}} 28^{\text{s}}$ ,  $\delta_{2000} = 59^{\circ} 16' 49''$ , and X-1 is within 7.5 arcsec of this position (see Figure 3). It is within 4.1 arcsec of the strongest ‘SNR candidate’ listed in table 3 of YS93. The H II region # 113 from Hodge & Lee (1990) has a central position of  $\alpha_{2000} = 00^{\text{h}} 20^{\text{m}} 27.7^{\text{s}}$ ,  $\delta_{2000} = 59^{\circ} 16' 50''$  (after making the correction described in Ohta et al. 1992), which is about 10 arcsec from the HRI centroid position. This H II region is extended and the catalogued H II regions in this area are underlain by widespread diffuse

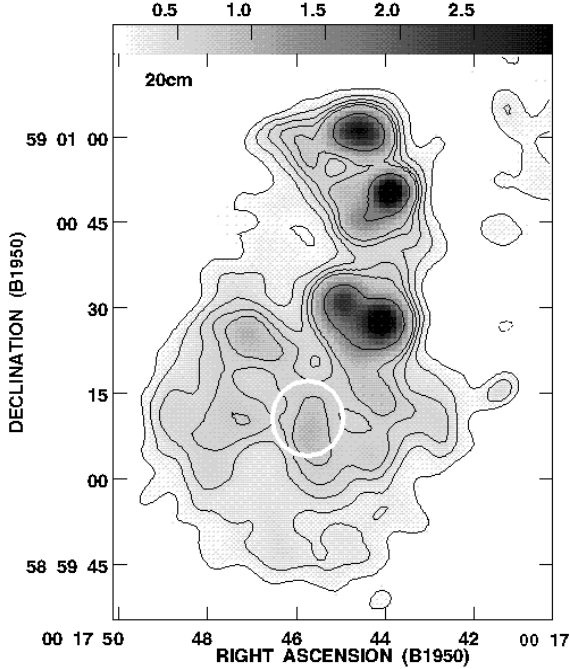


**Figure 3.** Radio continuum image at 20 cm of the YS93 non-thermal superbubble in IC 10 (from YS93). The HRI error region for X-1 is marked as a thick, white circle. The 1950 position for the centroid of X-1 is  $\alpha_{1950} = 00^{\text{h}} 17^{\text{m}} 45.9^{\text{s}}$ ,  $\delta_{1950} = 59^{\circ} 00' 11.9''$ . The dark, black regions show sites of thermal radio emission associated with known H II regions in IC 10. The less intense emission to the south is the YS93 non-thermal superbubble. See YS93 for details of the radio observations.

emission. In addition, the peculiar star WR17 from Massey & Armandroff (1995) is located at  $\alpha_{2000} = 00^{\text{h}} 20^{\text{m}} 29^{\text{s}}$ ,  $\delta_{2000} = 59^{\circ} 16' 52''$ , which is within 2 arcsec of the X-ray centroid. Massey & Armandroff (1995) give an optical spectrum of this star and classify it as a WN type Wolf-Rayet star based on the detection of a broad feature which they identify as He II 4686 Å. They find a  $V$  magnitude of 21.76 and  $E(B - V) = 0.77$ . Using the 3.5-m telescope of the Apache Point Observatory, we have performed independent optical spectroscopy which confirms that WR17 is an emission-line star of some type. The H $\alpha$  and [N II] emission lines of WR17 are systematically shifted by  $75 \pm 9 \text{ km s}^{-1}$  to the red compared to those of the aforementioned diffuse emission. This rules out the possibility that WR17 is a normal supergiant star with emission lines superimposed on it from the diffuse emission. The measured velocity for WR17 is  $-338 \text{ km s}^{-1}$ , and this agrees better with that of the surrounding H I than that of the H II. WR18 is also located within 6 arcsec of the HRI centroid, although Massey & Armandroff (1995) state that this is probably not a Wolf-Rayet star. Our independent spectroscopy suggests that WR18 may be an ordinary supergiant star with emission lines superimposed on it from the H II region.

#### *Confusing foreground and background sources*

IC 10 is at low Galactic latitude so confusing foreground sources are a natural concern. Based on results from the

*ROSAT* Galactic Plane survey (see section 9.1 of Motch et al. 1997), we expect about 0.9 sources per square degree with count rates as large as or larger than that of X-1. IC 10 has an angular size of about  $6.3 \times 5.1 \text{ arcmin}^2$ , so we estimate that there is less than about a 1 per cent chance of having a confusing foreground source this bright in front of IC 10. Furthermore, the HRI source is found at a position where one might expect X-ray activity in IC 10 based on its emission in other wavebands. For example, the X-ray source is almost exactly in the centre of the YS93 non-thermal superbubble (see YS93 for good arguments, but not rigorous proof, that the superbubble itself is in IC 10) and near a region of recent star formation. The superbubble has an angular size of about  $0.7 \times 0.7 \text{ arcmin}^2$ , so there is less than about a 0.02 per cent chance of having a confusing foreground source as bright as X-1 in front of it. We can further argue against some types of possible foreground sources based on examination of optical images. For example, we can use the nomograph shown in figure 1 of Maccararo et al. (1988) which relates the expected 0.3–3.5 keV X-ray flux to the visual magnitude for various types of astronomical objects. If we use the power-law model with a column of  $5 \times 10^{20} \text{ cm}^{-2}$  (see above), we predict a 0.3–3.5 keV flux of  $\approx 3.5 \times 10^{-13} \text{ erg cm}^{-2} \text{ s}^{-1}$ . There are no optical stars in the X-ray error circle with  $V$  magnitudes brighter than 20.8 (based on analysis of a  $V$  image taken with the 6-m telescope of the Russian Academy of Sciences), and thus from figure 1 of Maccararo et al. (1988) we see that the combined X-ray flux and  $V$  magnitude limit do not agree well with those expected from a normal foreground star (this is true even for 0.3–3.5 keV fluxes as low as  $\approx 1.9 \times 10^{-13} \text{ erg cm}^{-2} \text{ s}^{-1}$ ). Motch et al. (1997) state that about 85 per cent of their sources from the *ROSAT* Galactic Plane survey are stars with X-ray emitting coronae, so we have ruled out the most probable type of confusing foreground source. In summary, although we cannot formally prove that a foreground contaminating source is impossible, we consider one to be quite unlikely.

Confusing background sources (e.g. Seyfert galaxies, quasars and clusters of galaxies) are also unlikely. Examination of figure 18 of Motch et al. (1997) shows that the probability of having an extragalactic source as bright as X-1 behind the superbubble is  $\lesssim 1 \times 10^{-4}$ . This is a conservative probability estimate since any extragalactic source would also suffer from X-ray absorption by matter within the plane of IC 10. Some types of possible extragalactic confusing sources (e.g. clusters of galaxies) can also be ruled out based on the X-ray variability described below.

#### *Luminosity, spatial extent and variability*

Given that X-1 is probably located in the plane of IC 10, we expect that it will have some absorption over the Galactic column of  $3.2 \times 10^{21} \text{ cm}^{-2}$ . We expect an intrinsic column in IC 10 of  $\sim 2 \times 10^{21} \text{ cm}^{-2}$  based on figure 5 of YS93. We thus adopt a total column of  $5.2 \times 10^{21} \text{ cm}^{-2}$ . Using this column and a power-law model with a photon index of  $\Gamma = 2$ , we obtain a power-law normalization of  $3.5 \times 10^{-4} \text{ photons cm}^{-2} \text{ s}^{-1} \text{ keV}^{-1}$  at 1 keV. The 0.1–2.5 keV absorbed flux for this model is  $3.7 \times 10^{-13} \text{ erg cm}^{-2} \text{ s}^{-1}$ , and the 0.1–2.5 keV absorption-corrected flux is  $1.8 \times 10^{-12} \text{ erg cm}^{-2} \text{ s}^{-1}$ . While we note that the flux correction factor used above is

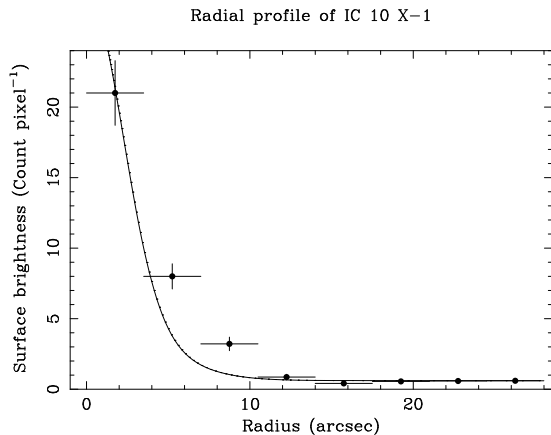


**Figure 4.** The data points show the HRI radial profile for IC 10 X-1. The background level of  $\approx 0.6$  count pixel<sup>-1</sup> is reached by a radius of  $\approx 14$  arcsec. The solid line shows the nominal HRI point spread function from section 2.2.3 of David et al. (1995). This point spread function has been normalized to the first data point for IC 10 X-1. Note that any X-ray extent is much less than the extent of the non-thermal radio superbubble. The small extent suggested by the data may well be entirely due to aspect solution errors (see the text for details).

large (about 4.9), the model we have used seems physically appropriate given the probable nature of X-1 (see below), and the presence of a large column between the plane of IC 10 and Earth is without question. At a distance of 1 Mpc the absorption-corrected flux corresponds to a mean isotropic luminosity of  $2.0 \times 10^{38}$  erg s<sup>-1</sup>. If, for comparison, we only use the Galactic column and neglect the probable absorption in IC 10 then we obtain a 0.1–2.5 keV absorption-corrected flux of  $1.2 \times 10^{-12}$  erg cm<sup>-2</sup> s<sup>-1</sup> and an isotropic luminosity of  $1.4 \times 10^{38}$  erg s<sup>-1</sup> (the power-law normalization and absorbed flux for this model are given above).

Inspection of the X-ray morphology of X-1 does not show any strong evidence for deviations from a circular shape. As the YS93 superbubble has an extent of  $\approx 45$  arcsec, we have examined the spatial extent of IC 10 X-1 (see Figure 4). IC 10 X-1 is much less extended than the radio emission from the superbubble. While the radial profile shown in Figure 4 is not formally consistent with the nominal point spread functions described in David et al. (1995), it is known that aspect solution errors can lead to a significant broadening of the profiles of point sources in some HRI observations (see the discussion in Morse 1994). We do not have enough counts to perform aspect error correction using the Morse code HRIASPCOR in FTOOLS, and TV Cas is too far off axis to be a useful comparison point source. The current data do not give strong evidence for spatial extent over that from a point source which suffers from aspect solution errors. Furthermore, the variability discussed below suggests that most of the X-ray flux originates from a compact region with an extent of less than  $\sim 1$  light day.

Count rates from *ROSAT* should be averaged over an integer multiple of the 400-s wobble period when used to search for rapid variability of cosmic X-ray sources (see Brinkmann et al. 1994; although note that the effects of the wobble are less serious for the HRI than the PSPC). We have used a source cell with a radius of 20 arcsec to extract

a light curve of X-1. We use 400-s bins and neglect partially filled bins. In Figure 5 we show part of this light curve where there is evidence for X-ray variability. The count rate from IC 10 X-1 appears to have dropped by over a factor of 2 within a day. We have calculated the Poisson probability that the variability is merely due to photon statistics, and it is less than  $1 \times 10^{-8}$ . Even taking into account issues such as those described in Press & Schechter (1974), the variability appears to be of high statistical significance. We have used a double panel format in Figure 5 for clarity because our observations are spread over 10.8 days, and there are no data in between the two panels shown in Figure 5. We have verified the variability shown in Figure 5 using two independent *ROSAT* analysis software systems. The mean background count rate in the source cell, computed using a large, nearby, circular, background cell, is  $\approx 1.5 \times 10^{-3}$  count s<sup>-1</sup> for the left panel and  $\approx 1.3 \times 10^{-3}$  count s<sup>-1</sup> for the right panel. We have verified that there is no positional error (e.g. a shift or rotation) that could be moving the source out of our source cell during the times shown in our right hand panel (see Figure 6). If we bin an image using only the data from the left hand panel, we can clearly see X-1 over the background level. However, if we bin an image using only the data from the right hand panel, we cannot see X-1 despite the fact that the right hand panel has twice as much exposure and a slightly lower background. There is evidence for variability similar to that shown in Figure 5 throughout our observation. The highest count rate observed is about twice the mean count rate, which corresponds to a 0.1–2.5 keV isotropic luminosity of  $\approx 4 \times 10^{38}$  erg s<sup>-1</sup>.

As discussed below, it appears likely that X-1 is an X-ray binary system in IC 10. Unfortunately, our data do not appear to provide strong constraints on the binary orbital period via periodic X-ray flux variations (e.g. eclipses). This is due partially to the low count rate, but also to the fact that our 32.7 ks of exposure is broken into numerous, small, separated blocks with durations between 1200–3000 s.

### 2.1.3 Other X-ray emission in IC 10

We have used PSS and the HRI point spread function to search our HRI field for any other X-ray point sources coincident with the extent of IC 10. We do not detect any point X-ray sources stronger than  $4.5\sigma$  within the extent shown in figure 5 of YS93. We do not detect any significant point sources near the maser sites, and we do not detect the radio continuum source described in section 3.3 of Argon et al. (1994). The *ROSAT* Standard Analysis Software System (SASS) reports a possible diffuse X-ray source at  $\alpha_{2000} = 00^{\text{h}} 20^{\text{m}} 18.6^{\text{s}}$ ,  $\delta_{2000} = 59^{\circ} 18' 50''$  with a positional error of 20 arcsec. Careful examination of the X-ray image and the SASS output shows that this source is not of high statistical significance in the current data (e.g. there are background fluctuations at almost comparable levels). However, the fact that the SASS X-ray source is within 12.5 arcsec of a bright radio source discussed in section 3.4 of Klein & Gräve (1986) suggests that it may well be real (note that some of the source labeling in section 3.4 of Klein & Gräve 1986 is incorrect). The SASS X-ray source is also quite close to two of the sources listed in table 1 of YS93. This is the location of an H I hole in IC 10 which may have been created by supernova events. The ‘best guess’ HRI count rate for this

source is  $\sim 8 \times 10^{-4}$  count  $s^{-1}$ . Further X-ray observations are needed to study this emission.

We have used PSS and the HRI point spread function to place upper limits on point sources at several representative positions in IC 10 that lie  $> 14$  arcsec from IC 10 X-1. The typical  $2\sigma$  upper limit is about  $3.0 \times 10^{-4}$  count  $s^{-1}$ . Using a  $\Gamma = 2$  power law with a column of  $4.2 \times 10^{21}$   $\text{cm}^{-2}$  (motivated by the Galactic column and figure 5 of YS93), this corresponds to an absorbed 0.1–2.5 keV flux upper limit of about  $1.3 \times 10^{-14}$  erg  $\text{cm}^{-2}$   $s^{-1}$  and an absorption-corrected 0.1–2.5 keV flux upper limit of about  $5.7 \times 10^{-14}$  erg  $\text{cm}^{-2}$   $s^{-1}$ . The isotropic luminosity upper limit is about  $6.4 \times 10^{36}$  erg  $s^{-1}$ . This upper limit is appropriate for X-ray sources that are extended on scales smaller than or comparable to that of the HRI spatial resolution (about 5 arcsec which corresponds to about 24 pc at the distance of IC 10). Thus, this limit can be applied to supernova remnants in the free-expansion or Sedov-Taylor phases (with ages  $\lesssim 5000$  yr), although many supernova remnants have luminosities lower than our upper limit (see table 3.2 of Charles & Seward 1995). Of course, it is possible that there are even more highly obscured X-ray sources in IC 10 (i.e. sources that suffer even stronger intrinsic absorption in IC 10 itself) with larger isotropic X-ray luminosities than the limit given above. A hard X-ray observation of IC 10 could search for such sources.

In order to search for diffuse emission from IC 10 (e.g. from a hot interstellar medium), we have carefully examined moderately smoothed and heavily smoothed HRI images. We have used both full-band HRI images as well as images made using only HRI channels 3–8 (this can help to maximize the signal-to-noise level; see section 2.4 of David et al. 1995). There does not appear to be any highly significant diffuse X-ray emission coincident with the optical or radio extents of IC 10. To obtain a characteristic constraint on the amount of large-scale diffuse emission, we consider a circular ‘source’ aperture centred at  $\alpha_{2000} = 00^{\text{h}} 20^{\text{m}} 16.2^{\text{s}}$ ,  $\delta_{2000} = 59^{\circ} 18' 23''$  with a radius of 100 arcsec. This aperture includes many of the H II regions of IC 10, and it does not include IC 10 X-1. The mean count rate density within this aperture is  $(4.72 \pm 0.14) \times 10^{-3}$  count  $s^{-1}$  arcmin $^{-2}$ . For comparison, a circular ‘background’ aperture that is located outside the extent of IC 10 (at  $\alpha_{2000} = 00^{\text{h}} 20^{\text{m}} 55.6^{\text{s}}$ ,  $\delta_{2000} = 59^{\circ} 23' 57''$  and with a radius of 112 arcsec) has a mean count rate density of  $(4.54 \pm 0.11) \times 10^{-3}$  count  $s^{-1}$  arcmin $^{-2}$  (this mean count rate density may be compared with the HRI background values listed in table 5 of David et al. 1995). Thus, after background subtraction, our source aperture has a residual mean count rate density of  $(1.8 \pm 1.8) \times 10^{-4}$  count  $s^{-1}$  arcmin $^{-2}$  (i.e. it is consistent with zero). Adopting the same spectral model as used above for point-source upper limits, we find a mean (absorbed) surface brightness of  $(7.8 \pm 7.8) \times 10^{-15}$  erg  $\text{cm}^{-2}$   $s^{-1}$  arcmin $^{-2}$ . Of course, this value is an average constraint on large-scale diffuse emission, and it cannot be used on a point-by-point basis.

#### 2.1.4 The possible all-sky survey detection of IC 10

IC 10 is listed (without discussion) in Boller et al. (1992) as having been detected during the *ROSAT* all-sky survey (RASS). Revision of the all-sky survey processing has led to an improved position for the RASS source of  $\alpha_{2000} =$

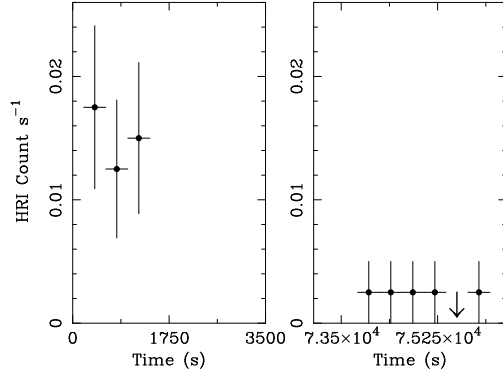


**Figure 5.** HRI light curve of IC 10 X-1 from part of our observation. Times are measured from 1996 January 18 16:13:20 UT. The light curve bin size is 400 s, and the two abscissae span the same length of time.

$00^{\text{h}} 20^{\text{m}} 21^{\text{s}}$ ,  $\delta_{2000} = 59^{\circ} 16' 18''$  (Th. Boller, private communication), and we show this position in Figure 1. The *ROSAT* Positional Sensitive Proportional Counter (PSPC; Pfeffermann et al. 1987) registered  $0.023 \pm 0.008$  count  $s^{-1}$  from the claimed all-sky survey source (Th. Boller, private communication), which corresponds to an equivalent HRI count rate of about  $8 \times 10^{-3}$  count  $s^{-1}$ . The all-sky survey exposure was short (494 s; Th. Boller, private communication) and places no useful spectral constraints on the PSPC source. Only about 13 PSPC photons in total (including background) were collected. The revised RASS position is 1.15 arcmin from our HRI position. The equivalent HRI count rate for the RASS source and our mean pointed HRI count rate for X-1 are similar, but the positional offset is somewhat larger than would be expected from the typical  $\approx 5$  arcsec HRI error circle radius and the typical  $\approx 40$  arcsec PSPC error circle radius. There are no HRI sources formally consistent with the RASS position, despite the fact that the HRI image probes much deeper than the RASS. Our position for X-1 is almost certainly not in error (see Figure 2 and the associated discussion), and the RASS data do not place a strong limit on the brightness of X-1 during the all-sky survey (X-1 lies between the 58 and 69 per cent contour levels for the RASS source).

## 2.2 NGC 147 and NGC 185

NGC 147 was observed with the HRI starting on 1995 January 19 (RH400744: total raw exposure of 14.8 ks spread over 63.6 ks), and NGC 185 was also observed starting on 1995 January 19 (RH400743: total raw exposure of 21.0 ks spread over 91.1 ks). Each observation had its pointing position coincident with the optical centre of the appropriate galaxy.

We have used PSS and the HRI point spread function to search for X-ray point sources coincident with these galaxies. We do not detect any X-ray sources coincident with the cores of these galaxies, and we do not detect any X-ray sources coincident with their known globular clusters either (we use the globular cluster positions from table 9 of Ford et al.

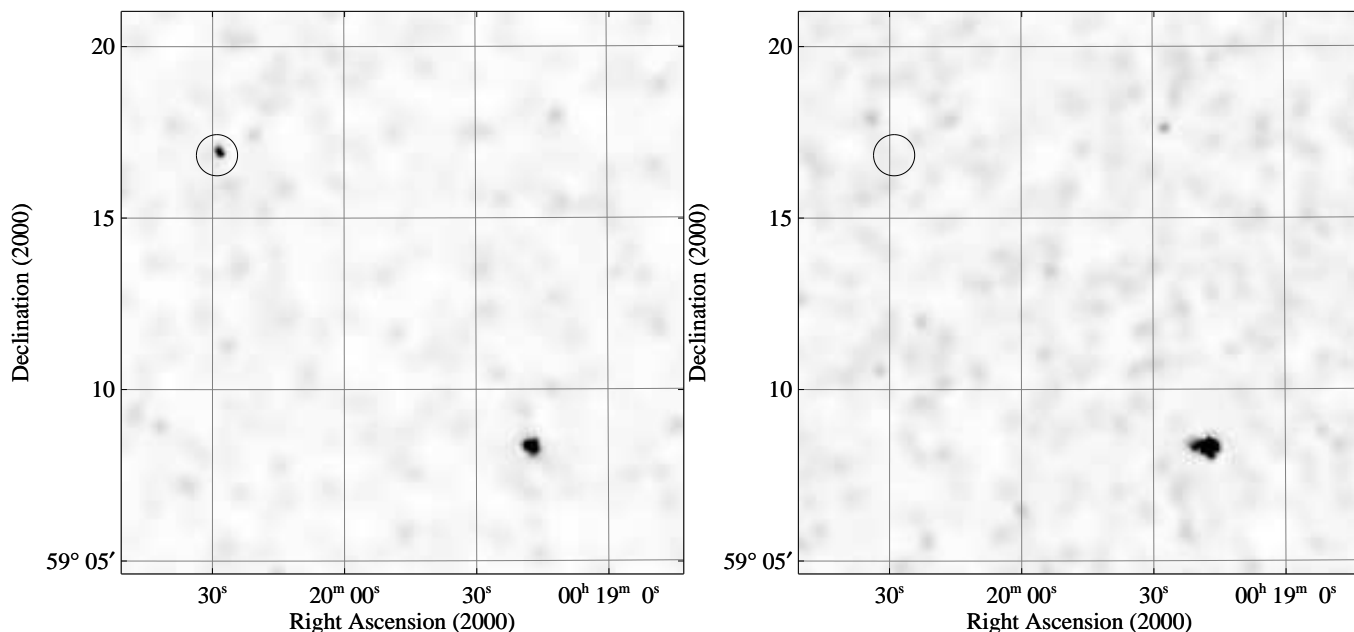


**Figure 6.** Smoothed HRI images illustrating the observed variability of X-1. X-1 is the circled source (the circle radius is arbitrary), and TV Cas is the source to the lower right. The left hand panel corresponds to the left hand panel of Figure 5, and the right hand panel corresponds to the right hand panel of Figure 5. The right hand panel has a longer integration time than the left hand panel, and the two images have the same (linear) scaling. Note that X-1 clearly varies in HRI count rate.

**Table 1.** X-ray sources near NGC 147 (the first three sources) and NGC 185 (the last two sources) in the HRI fields. Note that many of these sources are probably not related to NGC 147 or NGC 185 (see the text). The last column gives a brief description of the optical morphology based on inspection of Palomar Schmidt plates, Palomar 200-inch plates and Lick 3-m plates.

Source Number	$\alpha_{2000}$	$\delta_{2000}$	HRI count $s^{-1}$	Optical Morph.
1	00 32 10.6	48 33 40	$1.2 \times 10^{-3}$	Diffuse
2	00 32 28.3	48 31 56	$2.5 \times 10^{-3}$	Diffuse
3	00 34 02.1	48 23 38	$6.5 \times 10^{-4}$	Point source
4	00 38 21.9	48 24 09	$8.0 \times 10^{-4}$	See the text
5	00 39 02.3	48 24 15	$1.5 \times 10^{-3}$	Point source

1977). As with IC 10, we have scrutinized smoothed X-ray images of each of these galaxies and do not see any evidence for diffuse emission. We have placed upper limits on point sources at several representative positions in NGC 147, and the typical  $2\sigma$  upper limit is about  $6.0 \times 10^{-4}$  count  $s^{-1}$ . Using a  $\Gamma = 2$  power law with the Galactic column ( $1.2 \times 10^{21}$   $cm^{-2}$ ), this corresponds to an absorbed 0.1–2.5 keV flux upper limit of about  $2.3 \times 10^{-14}$  erg  $cm^{-2}$   $s^{-1}$  and an absorption-corrected 0.1–2.5 keV flux upper limit of about  $5.7 \times 10^{-14}$  erg  $cm^{-2}$   $s^{-1}$ . The isotropic luminosity upper limit is about  $2.3 \times 10^{36}$  erg  $s^{-1}$ . We have performed the same procedure for NGC 185, and the corresponding upper limits are  $4.6 \times 10^{-4}$  count  $s^{-1}$  (count rate),  $1.7 \times 10^{-14}$  erg  $cm^{-2}$   $s^{-1}$  (absorbed flux),  $4.3 \times 10^{-14}$  erg  $cm^{-2}$   $s^{-1}$  (absorption-corrected flux) and  $1.7 \times 10^{36}$  erg  $s^{-1}$  (isotropic luminosity).

In Table 1 we list all X-ray sources detected within 12 arcmin of the centres of NGC 147 and NGC 185. All of the sources in this table lie outside the central optical extents of NGC 147 and NGC 185, and all but source 5 lie outside the regions previously searched for globular clusters (see Baade 1951; Hodge 1974; Hodge 1976; Ford et al. 1977). However, these galaxies both are optically very large at faint surface brightness levels. Most of the X-ray sources in Table 1 are probably unrelated foreground or background sources, but a couple of them may be associated with these galaxies or currently unknown globular clusters. None of the sources in Table 1 is currently listed in the NASA Extragalactic Database (NED) or the SIMBAD database. We give optical morphologies of possible counterparts to the X-ray sources in Table 1. Source 4 is near the center of a ring of stellar images and there appears to be a very faint object about 2 arcsec southwest of the X-ray position. Source 5 is almost certainly not a globular cluster, as it is not resolved into stars on red Palomar plates. It appears to be a foreground star.

### 3 DISCUSSION AND SUMMARY

X-1 appears to be located in IC 10 near the centre of the YS93 non-thermal radio superbubble, and it has a powerful mean 0.1–2.5 keV isotropic luminosity of  $\approx 2 \times 10^{38}$  erg  $s^{-1}$ . Single (nondegenerate) stars do not produce this much X-ray emission (e.g. Rosner, Golub & Vaiana 1985; Pollock 1987; Kashyap et al. 1992; and references therein), and the X-ray luminosities of cataclysmic variables also fall short by several orders of magnitude (e.g. Eracleous, Halpern & Patterson 1991). The observed variability argues against most of the

emission coming from a cluster of stars or a supernova remnant. Thus it appears most likely that we have discovered an accreting neutron star or black hole in a binary system. The highest 0.1–2.5 keV luminosity we observe from IC 10 X-1 is  $\approx 4 \times 10^{38} \text{ erg s}^{-1}$ , and the total X-ray luminosity is likely to be  $\gtrsim 6 \times 10^{38} \text{ erg s}^{-1}$  if the source is indeed an accreting neutron star or black hole (see White, Nagase & Parmar 1995 for a discussion of the X-ray spectral energy distributions of X-ray binaries). This is the Eddington limit luminosity for a  $\approx 5 M_{\odot}$  object which is above the maximum mass for a neutron star. While this may suggest the compact object is a black hole, we cannot rule out a neutron star which emits anisotropically or at a super-Eddington rate. This is especially true in light of the low heavy element abundances in IC 10 (e.g. Lequeux et al. 1979) and the apparent X-ray luminosity/abundance relation for accreting compact objects (Clark et al. 1978; section 2.5 of van Paradijs & McClintock 1995).

As a peculiar emission-line star (WR17) has been located in the tiny HRI error circle by Massey & Armandroff (1995; see above), it is worth investigating whether this could be the binary companion star to the accreting compact object. If, as claimed by Massey & Armandroff (1995), this star is a WN type Wolf-Rayet star, then IC 10 X-1 would be a more X-ray luminous version of the possible Wolf-Rayet X-ray binaries reported near the centre of 30 Doradus (Wang 1995; also see van Kerkwijk et al. 1996 and references therein regarding the possible Wolf-Rayet nature of Cyg X-3). The system would have originally been a binary with two massive stars, and a supernova in this system would probably have contributed to the creation of the YS93 superbubble (such a system might plausibly remain bound after a supernova; see Brandt & Podsiadlowski 1995). Of course, the identification of X-1 with WR17 has not yet been proven and X-1 could also be a low mass X-ray binary in which the optical companion is below the current threshold of detectability (cf. Stocke, Wurtz & Kühr 1991; but note that Petre 1993 suggests that low mass X-ray binaries are rare in star forming regions).

Finally, the presence of a powerful X-ray source in the centre of an unusually large bubble of radio emission invites a brief comparison with SS433 and W50. YS93 compared the radio surface brightness ( $\Sigma$ ) and diameter ( $d$ ) of their superbubble to the so-called ‘ $\Sigma$ - $d$  relationship’ for SNR in the Magellanic Clouds. While the physical meaning, if any, of the  $\Sigma$ - $d$  relationship is somewhat obscure (especially when transported wholesale from the Magellanic Clouds to IC 10), the YS93 superbubble does appear to have a much larger diameter than expected given its radio surface brightness. YS93 proposed a multiple SNR model to explain this fact. While the YS93 model appears entirely plausible, W50 also lies off the  $\Sigma$ - $d$  relation (Margon 1984; its largest dimension is about 65 pc). The growth of the YS93 superbubble could have been influenced by IC 10 X-1 (see section 5 of Margon 1984). IC 10 X-1 does not appear to have redshifted/blueshifted emission lines in the spectrum of Massey & Armandroff (1995) and there is no strong radio point source at its position, so if there were SS433-like activity in the past it appears to have ended.

*ASCA* or *SAX* observations of IC 10 would be very useful as they would (1) probably obtain a significantly higher count rate from IC 10 X-1 due to the heavy column which

strongly affects the HRI band, (2) allow a better variability study including searches for eclipses from a high mass companion and X-ray pulsations, (3) allow a measurement of the spectral shape of IC 10 X-1 and (4) search for additional variable and highly absorbed X-ray sources in IC 10. They would also allow a much more precise determination of the luminosity of IC 10 X-1 since the column correction factor would not be so large. We are attempting to obtain such observations. We are also trying to search for evidence of a binary star (especially WR17) within the X-ray error circle and obtain higher quality spectra to further examine the Wolf-Rayet classification of WR17 by Massey & Armandroff (1995). Our current spectra do not allow definitive discussions of either of these issues.

If there are any X-ray binaries in the centres of NGC 147 or NGC 185, they were quite faint at the times of these observations (see Section 2.2 for upper limits). We do not detect the putative SNR of Gallagher et al. (1984), although our data do not rule out the possibility that this object is a SNR.

## ACKNOWLEDGMENTS

We gratefully acknowledge financial support from the Smithsonian Institution and the United States National Science Foundation (WNB) and the Royal Society (ACF). We thank H. Ebeling for the use of his IMCONT software, and we thank D. Zucker for reducing the optical spectra of stars in the region of IC 10 X-1. We thank Th. Boller, D. Harris, L. Ho, P. Massey, J. McClintock, P. O’Brien, R. Petre, Ph. Podsiadlowski and H. Yang for helpful discussions. The Palomar Schmidt plate image was obtained via the Digitized Sky Survey which was produced at the Space Telescope Science Institute under United States Government grant NAG W-2166. The Palomar Observatory Sky Survey was funded by the National Geographic Society.

## REFERENCES

- Allan D.J., 1995, *ASTERIX User Note 004: Source Searching and Parameterisation*. Univ. of Birmingham, Birmingham
- Argon A.L., Greenhill L.J., Moran J.M., Reid M.J., Menten K.M., Henkel C., Inoue M., 1994, *ApJ*, 422, 586
- Baade W., 1951, *U. Mich. Obs. Pub.*, 10, 7
- Baan W.A., Haschick A., 1994, *ApJ*, 424, L37
- Boller Th., Meurs E.J.A., Brinkmann W., Fink H., Zimmermann U., Adorf H.-M., 1992, *A&A*, 261, 57
- Brandt W.N., Podsiadlowski Ph., 1995, *MNRAS*, 274, 461
- Brinkmann W., et al., 1994, *A&A*, 288, 433
- Charles P.A., Seward F.D., 1995, *Exploring the X-ray Universe*. Cambridge University Press, Cambridge
- Clark G., Doxsey R., Li F., Jernigan G., van Paradijs J., 1978, *ApJ*, 221, L37
- David L.P., Harnden F.R., Kearns K.E., Zombeck M.V., 1995, *The ROSAT High Resolution Imager*. GSF, Greenbelt
- Eracleous M., Halpern J., Patterson J., 1991, *ApJ*, 382, 290
- Ford H., Jacoby G., Jenner D., 1977, *ApJ*, 213, 18
- Gallagher J.S., Hunter D.A., Mould J., 1984, *ApJ*, 281, L63
- Helfand D.J., 1984, *PASP*, 96, 913
- Hodge P.W., 1974, *PASP*, 86, 289
- Hodge P.W., 1976, *AJ*, 81, 25
- Hodge P.W., Lee M.G., 1990, *PASP*, 102, 26



Hodge P.W., 1994, in Munoz-Tunon C., Sanchez F., eds, *The Formation and Evolution of Galaxies*. Cambridge Univ. Press, Cambridge, p. 1

Kashyap V., Rosner R., Micela G., Sciortino S., Vaiana G.S., Harnden F.R., 1992, *ApJ*, 391, 667

Khalesseh B., Hill G., 1992, *A&A*, 257, 199

Klein U., Gräve R., 1986, *A&A*, 161, 155

Lequeux J., Peimbert M., Rayo J.F., Serrano A., Torres-Peimbert S., 1979, *A&A*, 80, 155

Maccacaro T., Gioia I.M., Wolter A., Zamorani G., Stocke J.T., 1988, *ApJ*, 326, 680

Margon B., 1984, *ARA&A*, 22, 507

Massey P., Armandroff T.E., Conti P.S., 1992, *AJ*, 103, 1159

Massey P., Armandroff T.E., 1995, *AJ*, 109, 2470

McGale P.A., Pye J.P., Hodgkin S.T., 1996, *MNRAS*, 280, 627

Metcalfe T.S., 1995, *IAU Inform. Bull. Var. Stars*, 4197

Minkowski R., Abell G.O., 1963, in Strand K., *Basic Astronomical Data*. Univ. Chicago Press, Chicago, p. 481

Morse J.A., 1994, *PASP*, 106, 675

Motch C., Guillout P., Haberl F., Pakull M., Pietsch W., Reinsch K., 1997, *A&A*, 318, 111

Mukai K., 1995, *PIMMS Users' Guide*. NASA/GSFC, Greenbelt

Ohta K., Sasaki M., Yamada T., Saito M., Nakai N., 1992, *PASJ*, 44, 585

Petre R., 1993, in Beckman J., Colina L., Netzer H., eds, *The Nearest Active Galaxies*. CSIC Press, Madrid, p. 117

Pollock A.M.T., 1987, *ApJ*, 320, 283

Pfeffermann E., et al., 1987, *Proc. SPIE*, 733, 519

Press W.H., Schechter P., 1974, *ApJ*, 193, 437

Rosner R., Golub L., Vaiana G.S., 1985, *ARAA*, 23, 413

Singh K.P., Drake S.A., White N.E., 1996, *AJ*, 111, 2415

Stark A.A., Gammie C.F., Wilson R.W., Bally J., Linke R., Heiles C., Hurwitz M., 1992, *ApJS*, 79, 77

Stocke J.T., Wurtz R., Kühr H., 1991, *AJ*, 102, 1724

Trümper J., 1983, *Adv. Space Res.*, 4, 241

van Kerkwijk M.H., Geballe T.R., King D.L., van der Klis M., van Paradijs J., 1996, *A&A*, 314, 521

van Paradijs J., McClintock J.E., 1995, in Lewin W.H.G., van Paradijs J., van den Heuvel E.P.J., eds, *X-ray Binaries*. Cambridge Univ. Press, Cambridge, p. 58

Wilson C.D., 1995, *ApJ*, 448, L97

Wang Q.D., 1995, *ApJ*, 453, 783

White N.E., Nagase F., Parmar A.N., 1995, in Lewin W.H.G., van Paradijs J., van den Heuvel E.P.J., eds, *X-ray binaries*. Cambridge Univ. Press, Cambridge, p. 1

Yang H., Skillman E.D., 1993, *AJ*, 106, 1448 (YS93)

large data gaps prevent a detailed X-ray variability analysis. Based on the count rate conversion factor in Singh et al. (1996) and the relative responses of the *ROSAT* PSPC and HRI, we estimate that 1 HRI count s<sup>-1</sup> corresponds to about  $3.0 \times 10^{-11}$  erg cm<sup>-2</sup> s<sup>-1</sup>. Using a distance of 275 pc (from table 7 of Khalesseh & Hill 1992), we calculate a 0.1–2.5 keV luminosity of about  $9 \times 10^{30}$  erg s<sup>-1</sup>, which suggests fairly typical coronal activity for an Algol-type binary.

## A2 BH Cas: W UMa-type binary

BH Cas is offset from the centre of the HRI field of view by about 11 arcmin, and we detect about 42 counts from it after background subtraction (the detection significance is  $5.4\sigma$ ). The count rate after correction for vignetting is  $1.4 \times 10^{-3}$  count s<sup>-1</sup>, and we are not able to probe for variability due to the low count rate. We adopt the same count rate to flux conversion factor as above and thus derive a 0.1–2.5 keV flux of  $4.2 \times 10^{-14}$  erg cm<sup>-2</sup> s<sup>-1</sup>. The distance to BH Cas is not well known, but an upper limit on the distance is  $530 \pm 70$  pc (T. Metcalfe, private communication). Thus the X-ray luminosity appears to be less than about  $1.3 \times 10^{30}$  erg s<sup>-1</sup>. The observed X-ray flux does not allow a strong constraint on the distance via the implied luminosity (compare the range of W UMa X-ray luminosities seen in McGale et al. 1996).

This paper has been produced using the Royal Astronomical Society/Blackwell Science L<sup>A</sup>T<sub>E</sub>X style file.

## APPENDIX A: BASIC X-RAY DATA FOR TV CAS AND BH CAS

In this appendix we give the first X-ray data on the serendipitously detected binaries TV Cas and BH Cas (see section 2.1.1). This will allow their inclusion in future systematic studies of the X-ray emission from Algol and W UMa-type binaries (e.g. Singh, Drake & White 1996; McGale, Pye & Hodgkin 1996; and references therein).

### A1 TV Cas: Algol-type binary

TV Cas is offset from the centre of the HRI field of view by about 12 arcmin, and we detect about 1080 counts from it after background subtraction (the detection significance is  $> 50\sigma$ ). The mean count rate after correction for vignetting is  $3.6 \times 10^{-2}$  count s<sup>-1</sup>, and there is evidence for count rate variability by a factor of about 2. The low count rate and